

Model-Based Sensor Design Optimization for UXO Classification

Robert E. Grimm and Thomas A. Sprott
Blackhawk GeoServices, 301 B Commercial Rd., Golden CO 80401
Voice 303-278-8700; Fax 303-278-0789; Email grimm@blackhawkgeo.com

Session 13: Detection, Including Discrimination

Abstract

The triaxial dipole response of model objects with various shapes, orientations, and depths was used to assess the relative merit of a number of candidate transmitter-receiver geometries for UXO discrimination. Targets included a sphere, a cylinder (UXO simulant), a disc, and two triaxial shapes intended to represent clutter or OE scrap. Sensor systems consisted of one or more transmitter coils up to 1-m diameter and various numbers of compact EM sensors. Sensors were placed within the transmitter and in its plane and some systems had a second plane of sensors above the transmitter. Synthetics were calculated with the sensor system sweeping a grid and with the system stationary near the target. After adding gaussian noise, the data were inverted for the principal polarizabilities $\beta_1, \beta_2, \beta_3$ and the ratios β_2/β_1 and β_3/β_1 were compared to the true values for each shape. We confirm that three-component (*xyz*) receivers are superior to a single (*z*) component and that only modest improvements in shape recovery are achieved with a second sensor plane when there is good coverage in one plane (e.g., a grid). The optimum configuration among those studied consisted of four adjacent 0.5-m transmitter coils with a single three-component sensor in the middle of each; the coils are powered in alternate countercirculating patterns as well as a same-sense pattern. This generates significant horizontal field so that all target axes are energized, improving discrimination. For a simple 1-m transmitter loop, nine three-component sensors in the transmitter plane appear to provide the best trade-off between performance and complexity: this resolves the secondary magnetic field without introducing excessive redundancy. Purely static configurations performed much more poorly, although the countercirculating pattern was able to partially offset these imposed geometric limitations. Development of a prototype field system will follow.

Introduction

Improved discrimination of UXO requires more sophisticated sensor systems than those in common use today. Among the pulsed-induction or time-domain electromagnetic (EM) systems, the Geonics EM61 and its UXO-specific modifications (e.g., MTADS, MTADS Man-Portable) are widely used and have proved to be effective at detection. While some ability for discrimination has been demonstrated with these systems (e.g., *Barrow and Nelson*, 1999; 2000), their potential is limited because they comprise a few, large coils recording the eddy current decay at a single time gate. The EM63 and EM61-MK2 extend the performance to recording multiple time gates, whereas the EM61-3D records multiple time gates in three spatial components. As part of our ongoing work to develop sensor platforms for improved UXO discrimination (*Wold et al.*, this volume), we carried out a model-based design study to attempt to find the best tractable design that could be field prototyped. Although more than a dozen

platform configurations were examined, the set is not exhaustive and further work may be necessary before hardware implementation.

Model

Our model builds on earlier work (see *McNeill and Bosnar, 1996; Barrow and Nelson, 1999, 2000; Pasion and Oldenberg, 2001*) of relatively simple models for UXO characterization. The target is treated as three orthogonal dipoles with one, two, or three independent axes (a sphere has one independent axis and an axisymmetric object has two). The incident magnetic field from a square transmitter loop is geometrically projected upon each of these axes depending on target position and orientation. The time-domain electromagnetic signal in each axis of the target is assumed to respond as

$$B = \beta(t+\delta)^{-\gamma}\exp(-\alpha t)$$

where α , β , γ , and δ vary for each independent axis. The dipole secondary fields from each target axis are evaluated at the receiver to form the complete response. A spherical target measured with a single-gate system (like the EM61) requires only 4 parameters whereas a fully time-dependent triaxial model requires 18 parameters.

The inverse problem for target shape and orientation is solved through a generalized inverse using singular-value decomposition. Programmed options for conjugate-gradient, evolutionary-program, genetic-algorithm, or grid-search solutions were found to be no more effective than the generalized inverse for these data. However, a multi-step “recipe” was generally the most effective:

1. Obtain preliminary estimates of the order-of-magnitude of the intrinsic target parameters (here, just β) by assuming it is a sphere (one independent axis only; solution is for position and one set of time parameters).
2. Copy these estimates to the other axes and re-solve for target with 3 independent axes.
3. If the largest β value is not the 1-axis, exchange these values and re-solve for orientation, holding all other parameters fixed.

The time-domain response decreases sharply with time and also varies in strength with spatial component: Z is typically larger than X or Y . In order to balance all of the data in the least-squares inversion, both time- and component-equalization was applied by normalizing each time channel and component by the its RMS value

This model has been very successful in recovering the shape of buried targets probed with the EM61-3D: a neural network trained on the intrinsic model parameters (three each α , β , γ , δ) estimated from 26 targets in 50 depth-orientation states yielded a 96% probability of detection at 30% false alarms in discriminating cylindrical (UXO-like) targets from other objects. We attribute the relative success of the EM61-3D compared to other sensors to its measurement of three spatial components at multiple times during eddy-current decay; extension of these principles to multiple, compact sensors is the focus of this effort. Preliminary modeling of data acquired with a vector multisensor array are discussed by *Wold et al.* (this volume).

System Optimization

The general problem of an “optimal” EM system for UXO discrimination involves trade-offs of the number, size, position, and orientations of the transmitters and receivers, the transmitter

pulse shape and repetition rate, and the number, spacing, and width of receiver time gates. Our approach to optimization is to calculate a large number of forward models with different targets and sensor-platform configurations, and then to invert these synthetic data for the target parameters; the quality of how well diagnostic parameters are recovered indicates the quality of the sensor platform. Here we consider transmitter coil configurations 1-m square (so as to be man-portable) with one- (Z) or three- (XYZ) component receivers within the column circumscribed by the transmitter coil. Eleven such configurations are shown below in Figure 1, along with four existing systems: MTADS, EM61, EM61-3D and EM63 (the last is denoted EM61-1C).

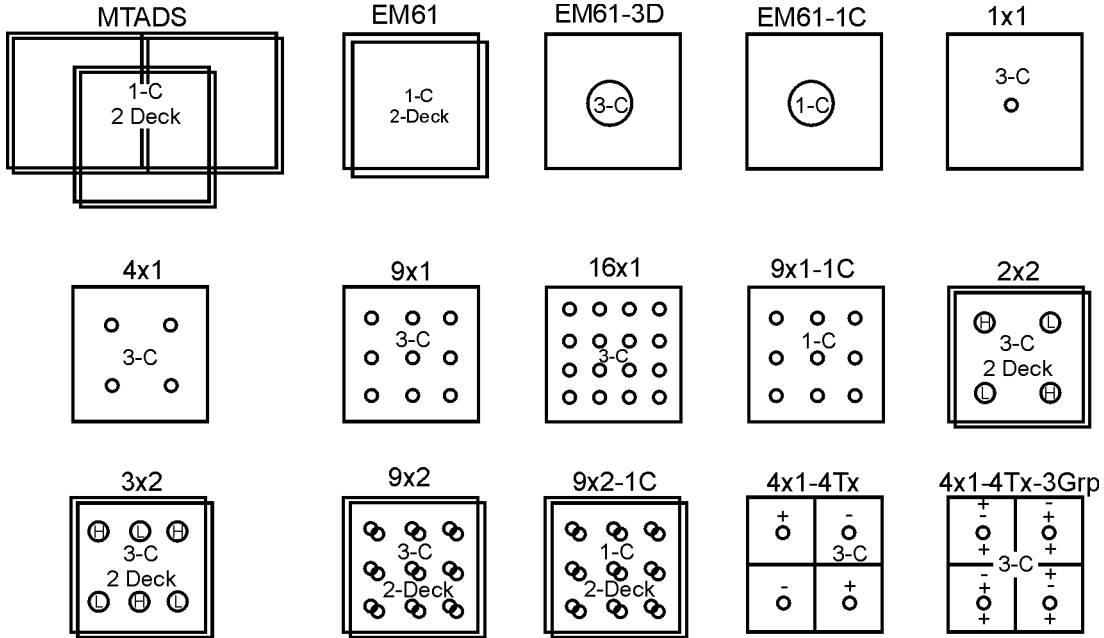


Figure 1. EM transmitter/receiver configurations considered for design study. Standard transmitter is 1-m diameter and 0.4-m above ground level. “1-C” indicates receiver is one-component (vertical) field only; “3-C” is full vector field. “2 Deck” indicates receivers are in the transmitter plane and in a second plane 0.4-m higher. “L” and “H” show receiver positions on two decks where they are not vertically superimposed. Plus and minus signs on the last two configurations indicate countercirculating currents in adjacent, smaller coils, used to generate a more complex source field from planar coils.

Also for this preliminary effort, we only examined the leading geometrical (spatial) effects of these platforms without regard to temporal effects, so the model responses are evaluated and inverted only for the three β parameters along with position and orientation.

The targets modeled for this study, and their specified three-axis β ratios, were:

- (1) Sphere 1:1:1
- (2) Cylinder (UXO simulant) 8:1:1
- (3) Disc 64:64:1
- (4) Book-1 (to be distinguished from UXO) 11:6:1
- (5) Book-2 (155-mm scrap simulant) 45:5:1

The “book” shapes are triaxial like their namesakes; all others are axisymmetric. All of the target β s were rescaled to have the same geometric mean value, thus ensuring that the mean response amplitudes would be the same. Target depths of 0.15, 0.5, and 1 m were modeled;

because shape recovery was markedly poorer overall at 1 m, these results are excluded here. Nine orientations were modeled with azimuth and inclination distributed over a quarter-sphere (all that is needed for a dipole). Gaussian noise was added to the forward models with standard deviation equal to a specified fraction of the signal for each platform from the cylinder in the vertical orientation at the shallowest depth studied. Five noise levels from 0-3% were evaluated; note that the actual noise in most of the cases is much worse than suggested by the level designations, because the response of the shallow vertical cylinder was selected as being the largest against which to scale other configurations. For example, the noise level for the signal-to-noise for the reference vertical cylinder at 0.15-m depth is nearly 100x larger than a horizontal cylinder at 0.5-m depth. The variations of sensor platform, target type, depth, orientation, and noise required some 10,000 forward and inverse models. Data were “acquired” in two modes. First a high-density grid of 360 points in a 2x2-m area over each target was intended to simulate the kind of dynamic data that could be taken and accurately positioned with an inertial navigation system. At the other extreme, a single position over the middle of the target box was selected, representing the simplicity of a static array. Lane-style data (i.e., line-station) represent an intermediate case that has not yet been considered.

Discrimination between different targets was assessed by plotting the true and estimated values of β_2/β_1 vs β_3/β_1 . These ratios provide indicators of shape alone without regard to target size. The estimated fits were evaluated by the sum of the absolute differences in the logarithm of the β -ratios:

$$\text{Error} = \text{abs}[\log_{10}(\beta_2/\beta_1)_{\text{pred}} - \log_{10}(\beta_2/\beta_1)_{\text{true}}] + \text{abs}[\log_{10}(\beta_3/\beta_1)_{\text{pred}} - \log_{10}(\beta_3/\beta_1)_{\text{true}}]$$

In order to condense the results for different orientations and depths into a single statistic, the 70th percentile of the errors for each target were reported; this would correspond to approximately 1 standard deviation if the results were drawn from a normal distribution.

Dense-grid acquisition at zero noise (Figure 2) results in perfect shape recovery of the sphere, cylinder and book-1 shapes for most of the sensor-platform designs (bottom 2 rows of Fig. 2). There is some scatter in β_3/β_1 for the disc and book-2 shape that is due to the difficulty of the inversion in accurately recovering extreme aspect ratios (informally, they are very thin compared to their long dimensions). However, the EM61 family shows much more scatter even under these ideal conditions; the larger receiver coils do not resolve spatial variations in the EM field that improve discrimination. Note that the relatively good performance of the MTADS in this study cannot be achieved in practice because the towed array cannot be accurately positioned at hundreds of distinct points near the target. The result does illustrate the value of a large transmitter than can “illuminate” the target from different angles.

At “3%” noise (Figure 3), there is much more variability in shape recovery for all platforms, but several trends can be discerned which are summarized below. The key result is that that the countercirculating current systems in a four-coil transmitter group with four three-component receivers provided the best overall discrimination of those configurations studied. If this system is too complex to field, then a 4x4 or 3x3 grid of three-component receivers in the transmitter plane is still good. Again note that multiple small sensors are still preferable to the large EM61 receiver coils: in practice, the larger integration area of the latter may improve signal-to-noise relative to the small sensors but this effect is not evident here because the noise is self-scaled in each platform. Shape recovery under even noise-free static acquisition (Figure 4) was poor in general.

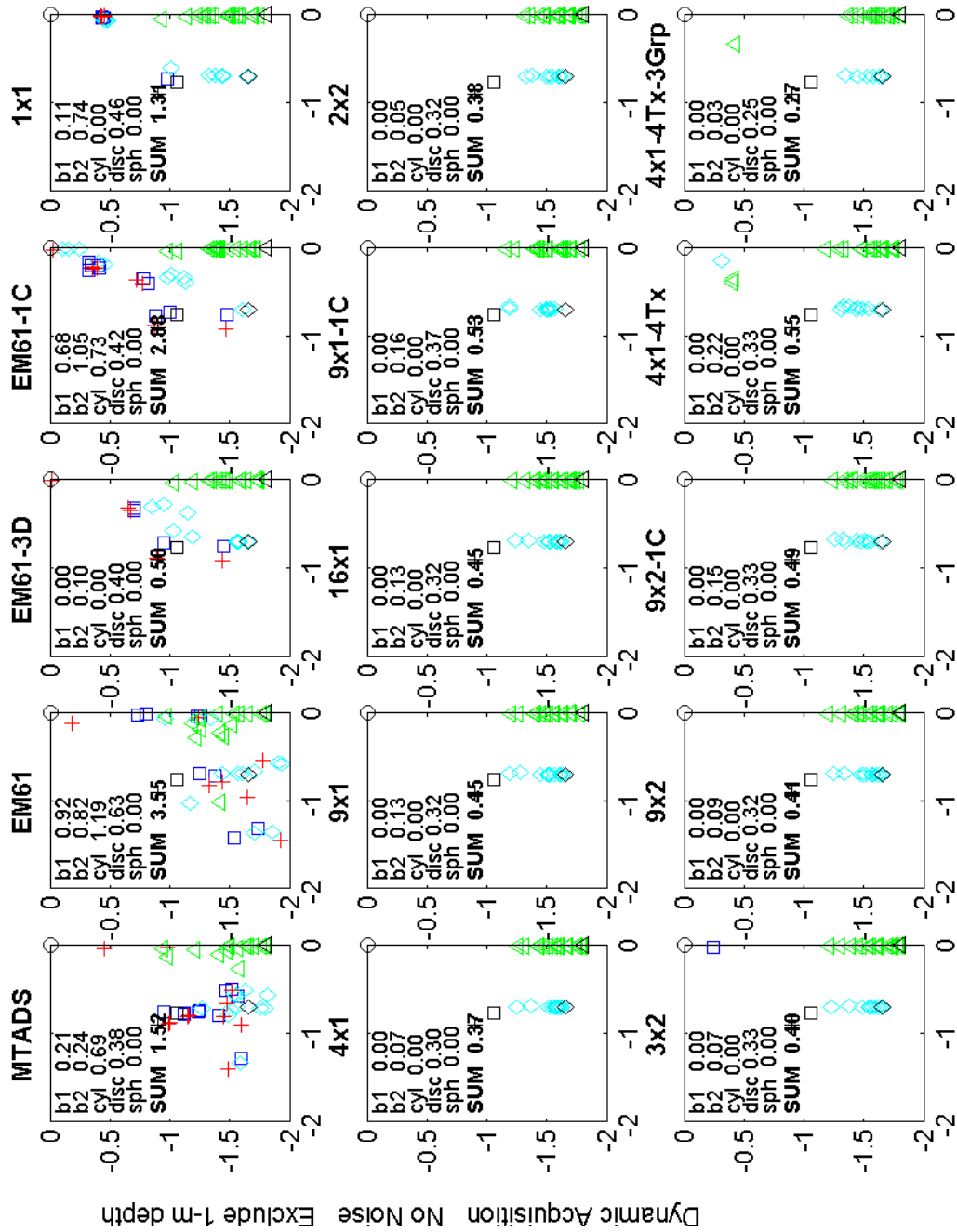


Figure 2. Shape estimation for noise-free synthetic data for 5 targets at 0.15 and 0.5-m depth. See previous figure for descriptions of sensor platforms. X-axis is $\log_{10}(\beta_2/\beta_1)$ and Y-axis is $\log_{10}(\beta_3/\beta_1)$. Magenta circle = Sphere, Red cross = Cylinder, green triangle = Disc, blue square = Book-1, cyan diamond = Book-2. The scatter in each shape is for the 18 different combinations of depth and orientation tested. True shape parameters are black symbols and are (0,0), (-0.9,-0.9), (0,-1.8), (-0.76,-1.06), and (-0.7,-1.65), respectively, for the Sphere, Cylinder, Disc, Book-1, and Book-2. Tabulated values are 70th percentile in error statistic (see text); lower values are better fits.

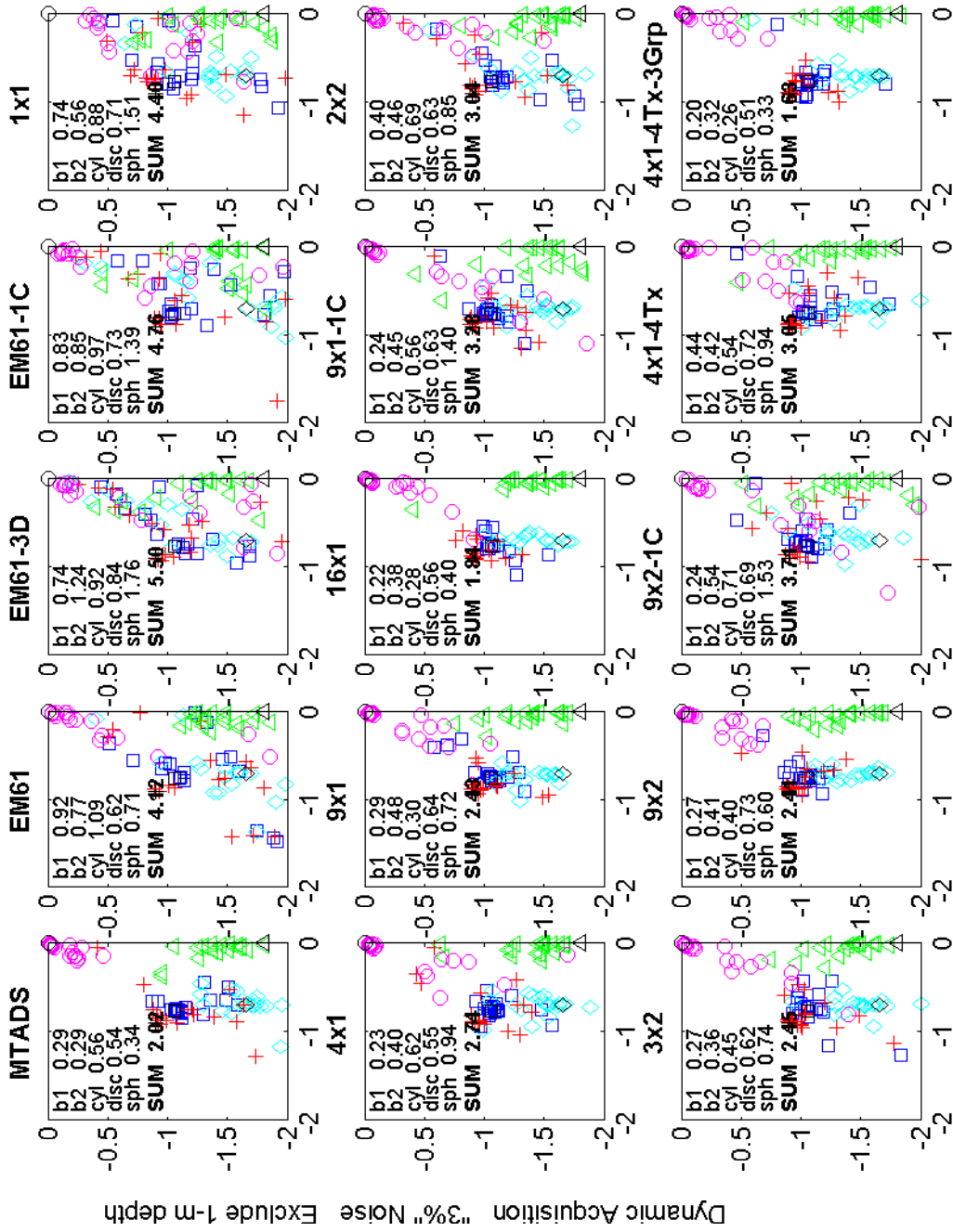


Figure 3. As Figure 2, but for gaussian noise with standard deviation equal to 3% of the largest signal generated for each configuration (a vertical cylinder at 0.15-m depth).

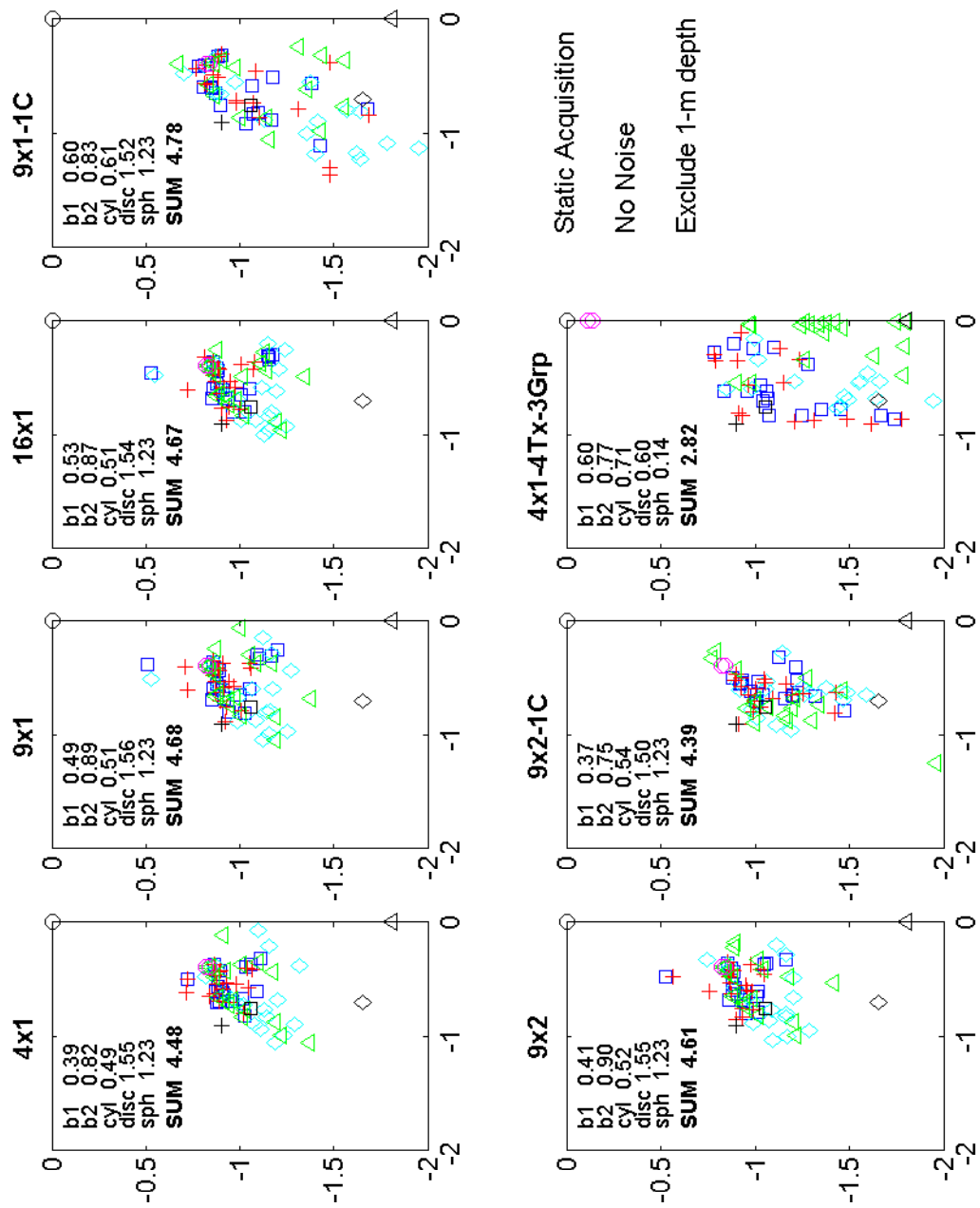


Figure 4. A restricted set of runs with data acquired only at a single point over the target. Note much poorer performance than when data are gathered over an area.

Conclusions

The results of this preliminary study show a general trend toward better shape discrimination with more sophisticated transmitter and receiver configurations; however, statistical variations in these moderate-sized samples may still preclude an absolute ranking. Nonetheless, several general conclusions can be made:

- (1) Three-component receivers are superior to a single (z) component.
- (2) Only modest improvements in shape recovery are achieved with a second sensor plane when there is good coverage in one plane (e.g., a dense grid).
- (3) The optimum configuration studied consisted of four adjacent 0.5-m transmitter coils with a single three-component sensor in the middle of each; the coils are powered in alternate countercirculating patterns as well as a same-sense pattern. This generates significant horizontal field so that all target axes are energized, improving discrimination
- (4) For a simple 1-m transmitter loop, nine three-component sensors in the transmitter plane appear to provide the best trade-off between performance and complexity: this resolves the secondary magnetic field without introducing excessive redundancy.
- (5) Purely static configurations (where the sensor platform is fixed at one position approximately over the target; not shown here) performed much more poorly (“*I’m better when I move*”), although the countercirculating pattern was able to partially offset these imposed geometric limitations.

We will extend this study to provide a more comprehensive evaluation of the system trade-offs necessary to optimize a standoff sensor platform for UXO characterization, including the number of xy data required, arbitrary 3D xyz data, true horizontal-field transmitters, the inclusion of temporal parameters, the statistical improvement for a larger number of depth-orientation states, and better discriminant statistics.

References Cited

- Barrow, B.J., and H.H. Nelson (1999). Model-based characterization of EM induction signatures for UXO/clutter discrimination using the MTADS Platform. *UXO Forum 1999*, CD-ROM.
- Barrow, B.J., and H.H. Nelson (2000). Analysis of magnetic and EMI signatures from impacted, intact ordnance and exploded fragments. *UXO/Countermine Forum 2000*, CD-ROM.
- McNeil, J.D., and M. Bosnar (1996). Application of time domain electromagnetic techniques to UXO detection, *UXO Forum 96*, pp. 34-42.
- Pasion, L.R., and D.W. Oldenburg (2001). A discrimination algorithm for UXO using time domain electromagnetics, *J. Env. Eng. Geophys.*, 6, 91-102.
- Wold, R., R. Grimm, M. Tondra, A. Jander, D. George, and A. Becker, Detection and Classification of UXO Using Multidimensional EM Sensors, *UXO/Countermine Forum 2002*, this volume.

Acknowledgements

We are grateful for support for this work from NAVEODTECHDIV, Indian Head, MD, Contract #N00174-98-0026 (PI R. Wold). Tom Bell kindly provided modeled β -values for 155-mm scrap.